Available online at www.sciencedirect.com

SciVerse ScienceDirect

Ceramics International 39 (2013) 8527–8530

CERAMICS INTERNATIONAL

www.elsevier.com/locate/ceramint

Short communication

Effects of Ni doping on ferroelectric and ferromagnetic properties of $Bi_{0.75}Ba_{0.25}FeO_3$

R. Castañeda[a], G. Rojas-George[b], J. Silva[c], M.E. Fuentes-Montero[a], J.A. Matutes-Aquino[b], A. Reyes-Rojas[b], L. Fuentes[b,*]

[a]Universidad Autónoma de Chihuahua, Chihuahua, Mexico
[b]Centro de Investigación en Materiales Avanzados S.C., Chihuahua, Mexico
[c]Universidad Autónoma de Ciudad Juarez, Chihuahua, Mexico

Received 18 December 2012; received in revised form 5 March 2013; accepted 15 March 2013
Available online 26 March 2013

Abstract

Variants of Ni-added $Bi_{0.75}Ba_{0.25}FeO_3$ (BBFO) multiferroic ceramic were prepared by the sol–gel method. The first variation line was the synthesis of $Bi_{0.75}Ba_{0.25}Fe_{1-x}Ni_xO_3$ ($x=0$, 0.025) solid solutions. The second variation was the preparation of BBFO impregnated with nickel oxide. Synthesized materials were characterized by x-ray diffraction (XRD) and scanning electron microscopy (SEM). Ferroelectric and ferromagnetic measurements were conducted as well. XRD data suggest the coexistence of a rhombohedral and a tetragonal phase when Ba^{2+} and Ni^{2+} cation substitutions are present. Ni acts as an inhibitor of grain growth and coalescence. After sintering, it reduces the average size from 88 nm to 67 nm. Furthermore, the presence of the Ni^{2+} cation in the $Bi_{0.75}Ba_{0.25}Fe_{0.975}Ni_{0.025}O_3$ octahedral position increases the saturation magnetization and suppresses the leakage current, which dampens the ferroelectric character of the non-doped perovskite family of BBFO. The Ni-doped BBFO ceramic achieves an interesting compromise between ferromagnetic and ferroelectric properties.

Keywords: A. Sol–gel processes; C. Ferroelectric properties; C. Magnetic properties; D. Perovskites

1. Introduction

$BiFeO_3$ (BFO), a prototype multiferroic, combines ferroelectric and characteristic (spin cycloid) antiferromagnetic orders above room temperature [1]. Consistently with its rhombohedrally distorted perovskite structure (space group R3c), BFO shows some degree of magnetoelectric coupling as well [2]. A drawback that limits BFO applications is its relatively significant electrical conductivity. The electromagnetic performance of this ceramic can be increased through cation doping into the A or B perovskite sites. $Bi_{0.75}Ba_{0.25}FeO_3$ (BBFO) has been demonstrated to be an excellent candidate to increase the ferromagnetic effect, with an acceptable ferroelectric response [3]. Furthermore, barium also reduces the leakage currents [4]. The results regarding the effect of Ni doping are controversial. According to [5], doping B-site with 2.5% Ni reduces the leak currents. On the other hand, [6] reports the opposite effect.

In the present work, in order to elucidate the just-mentioned point and in an effort to refine the properties of the considered family of materials, three different types of samples were synthesized and analyzed:

1) BBFO (without Ni doping)
2) Ni-doped BBFO ($Bi_{0.75}Ba_{0.25}Fe_{0.975}Ni_{0.025}O_3$ solid solution)
3) BBFO impregnated with Ni 2.5% (mixture≠solid solution). This material simulates unsuccessful synthesis of Ni-doped BBFO.

The ferroelectric and ferromagnetic behaviors of the considered materials are investigated.

2. Experimental

$Bi_{0.75}Ba_{0.25}Fe_{1-x}Ni_xO_3$ (BBFO, with $x=0$, 0.025) nanometric perovskite powders were synthesized by the Pechini method.

*Corresponding author. Tel.:+52 6144391159.
E-mail addresses: luis.fuentes@cimav.edu.mx, luis.fuentes.25.@gmail.com (L. Fuentes).

0272-8842/$ - see front matter © 2013 Elsevier Ltd and Techna Group S.r.l. All rights reserved.
http://dx.doi.org/10.1016/j.ceramint.2013.03.055

First, deionized water in a 761:1 M ratio of H_2O:BBFO was heated at 45 °C, with stirring and a reflux constant. Afterwards, 3.6:1 M ratio citric-acid:BBFO was added. A stoichiometric amount of iron nitrate monohydrate $Fe(NO_3)_3$•$9(H_2O)$ (Fisher Scientific, 99%) was added to the solution and dissolved for 15 min. Bismuth nitrate pentahydrate $Bi(NO_3)_3$•$5H_2O$ (Alfa Aesar, 98%) was added and dissolved for 2 h. Barium nitrate $Ba(NO_3)_2$ (Fisher Scientific, 99.3%) and nickel nitrate hexahydrate $Ni(NO_3)_2$•$(6H_2O$ (Fisher Scientific, 99.9%) were added and dissolved for 1 h. Next, 15:1 molar ratios ethylene-glycol: BBFO and 18:1 acetic-acid:BBFO were added to the aimed composition. As the final step, the solution mixture was stirred vigorously for 2 h.

Once the desired compositions were achieved, the gels were obtained at the same temperature over long time periods by slow evaporation. The resulting gels were dried at 100 °C and annealed at 600 °C for 60 min. BBFO undoped powders were impregnated with a Ni^{2+} nitrate solution in the same proportion as that of the Ni-doped perovskite (2.5%) and then the impregnated sample was again annealed at 600 °C for 60 min.

All the obtained powders were ground with PVA, pressed into pellet shapes and sintered from 845 °C to 860 °C for 90 min.

Phase and structure analyses were performed by XRD using a Panalytical XPert'PRO diffractometer, with Cu Kα monochromatic radiation and θ–2θ geometry. The microstructure and the grain size distributions were observed using a 30 kV field emission SEM, model JSM-7401F, JEOL. The ferroelectric effect in the samples was measured using a ferroelectric tester (Radiant Technologies Inc.). The polarization vs electric field (*P*–*E*) hysteresis loops were obtained at 100 Hz (300 K). The ferromagnetic loops of the samples were recorded using a PPMS (Quantum Design) with a VMS probe, at room temperature (300 K).

3. Results and discussion

Fig. 1 shows the samples' XRD patterns after sintering. The pure and the Ni-doped BBFO samples produced typical perovskite spectra [7,8], with neither secondary phases signals nor resolved peak splitting. Peaks' broadening is apparent, due to the small crystallite size, heterogeneous strains and plausibly local departures from cubic symmetry. The asymmetry of the (200) peak, pointed by an arrow in Fig. 1 inset (A), suggests the presence of a tetragonal phase in samples 1 and 2. Diffraction maxima in sample 2 patterns show a small displacement to the left. This is due to the partial substitution of Ni^{3+} (r=0.70 Å) in Fe^{3+} (0.67 Å) six-fold coordination sites. Naturally, Ni-impregnated sample 3 does not show the mentioned displacement. As this last-mentioned sample has been driven by further heat treatments, crystal growth has been better and diffraction peaks are somewhat sharper. Nevertheless, maxima's splitting is not observable. However, Ni impregnated BBFO perovskite was partially destabilized by the nucleation and growth of the $NiFe_2O_4$ (φ) spinel structure. This was to be expected, because the NiO acts as a destabilizing agent, which provokes Bi_2O_3 loss. BaO (β), $NiFe_2O_4$ (φ)

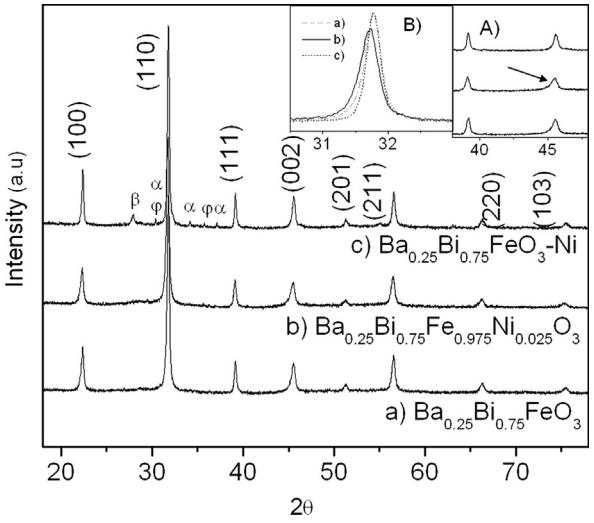

Fig. 1. XRD patterns of BBFO ceramics sintered at 845 °C. Sample 1—undoped BBFO. Sample 2—Ni-doped BBFO. Sample 3—Ni-impregnated perovskite. Secondary phases: α=$BaFe_{12}O_{19}$; β=BaO; and φ=$NiFe_2O_4$. Cubic indexing of peaks. The inset (A) describes in detail the (111) and (200) maxima. Splitting of (111) (not observed) would imply rhombohedral symmetry. The shoulder in (200) suggests the presence of a tetragonal phase. Inset (B) shows peak displacement due to Ni substitution.

and $BaFe_{12}O_{19}$ (α) precipitation are induced as well (see Fig. 1).

The BBFO microstructural analysis is shown in Fig. 2a and b, in a fracture zone cross-section. In this figure, the microstructure and porosity size can be observed. The crystal size distribution, obtained from SEM images and fitted by a log-normal distribution function, shows the geometric mean crystallite sizes around (88 ± 1) nm (Fig. 2c) and (67 ± 1) nm (Fig. 2d), for the BBFO and Ni doped samples respectively. Here, the Ni cation acts as a grain size inhibitor. This is consistent with results for Ni-doped BFO films described by other authors [9]. It has also been reported [10] that, as the BFO crystal size decreases from 95 nm to 14 nm, the magnetization response increases. This feature will be commented on below. As can be seen in Fig. 2, there is some porosity in the samples after the sintering process. The porosity originates in the fabrication process, plausibly from the carbon in polyvinyl alcohol (used when the powders are pressed into pellet shapes and sintered at 845 °C). The densities of the samples were 6.3 g/cm^3, 7.0 g/cm^3 and 7.4 g/cm^3 for the impregnated, undoped and Ni-doped samples respectively. Observed density variations are as expected.

The ferroelectric hysteresis loops (*P*–*E*) obtained at room temperature for all the samples are shown in Fig. 3. The saturation condition is not reached in any of them. The non-doped samples (BBFO and BBFO impregnated with NiO) have a leakage current profile behavior which is consistent with the results obtained by other authors [11]. However, in the Ni doped perovskite the conductivity is not so high. Most probably, the resistivity increment is due to $Fe^{3+} \rightarrow Fe^{2+}$ reduction in the vicinity of oxygen vacancies. Another factor that may increase the resistivity is the increment of boundary area as a side-effect of nickel-induced grain growth inhibition.

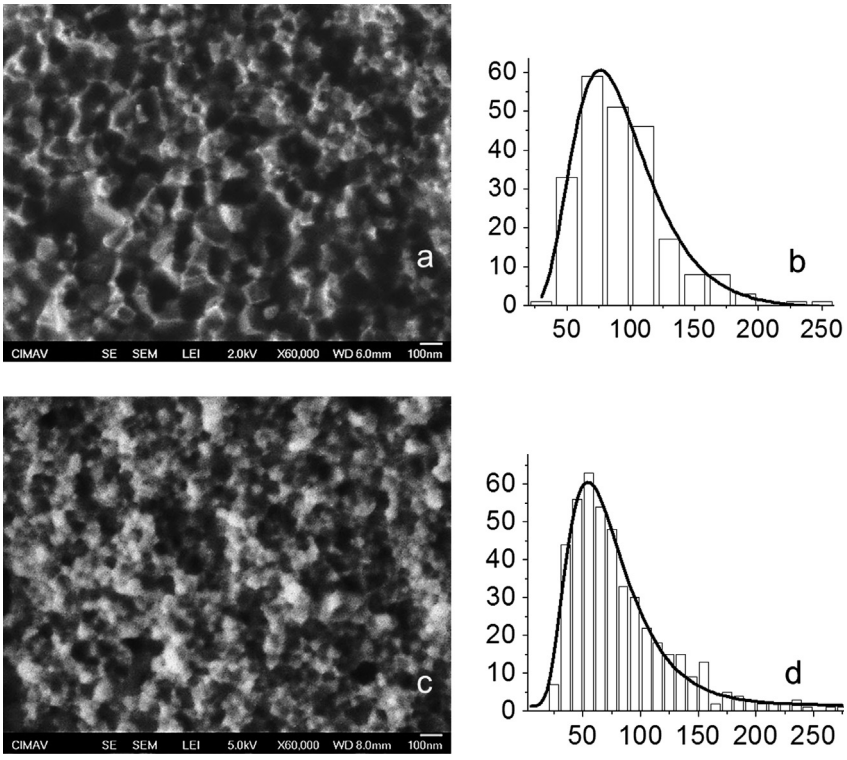

Fig. 2. (a,b) SEM image and size distribution of $Bi_{0.75}Ba_{0.25}FeO_3$ (c,d) SEM image and size distribution of $Bi_{0.75}Ba_{0.25}Fe_{0.975}Ni_{0.025}O_3$ respectively.

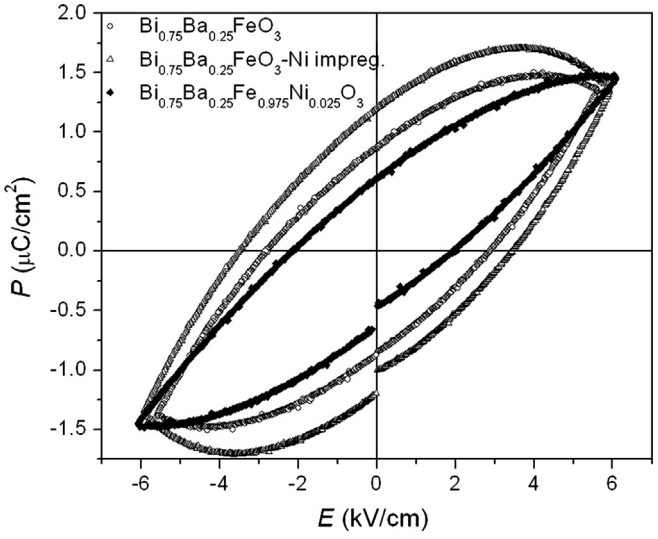

Fig. 3. Ferroelectric hysteresis loops at room temperature of all the samples.

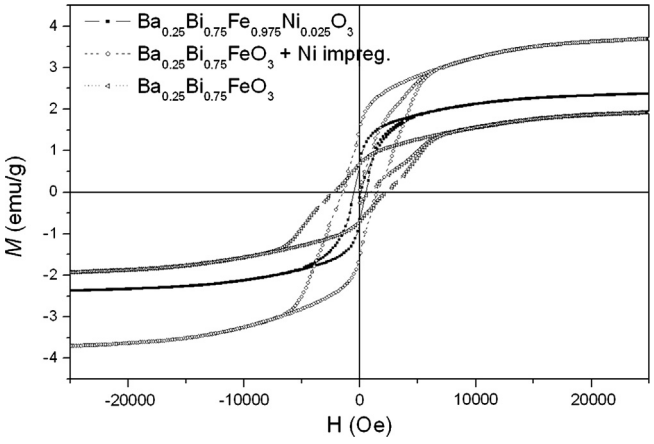

Fig. 4. Magnetic hysteresis loops at room temperature of all the samples.

Regarding remanent polarization, the Ni doped BBFO has a lower value (0.63 μC/cm^2) than that of the BBFO (0.87 μC/cm^2).

The magnetization curves obtained after the sintering process, as a function of the applied magnetic field (at room temperature), are shown in Fig. 4. These hysteresis magnetic (*M–H*) loops show the qualitative differences between these ceramics. The one corresponding to BBFO without Ni-doping shows a slight increase of the maximum magnetic saturation (1.9 emu/g) and the remanent magnetization (0.7 emu/g), with respect to the ones reported in other works, where the ceramics were synthesized by the conventional solid state reaction technique [12]. When the solid solution perovskite is doped with Ni cations, the remanent magnetization is the same, but the maximum magnetic saturation increases to 2.3 emu/g and the coercivity decreases to 0.54 kOe (four times smaller than without Ni, 2.3 kOe). However, when the perovskite is NiO impregnated, the maximum magnetic saturation reaches 3.7 emu/g, and the remanent magnetization is as high as 1.5 emu/g. This magnetization increment is presumably due to the secondary phases contained in this ceramic; the NiO impregnation produces $BaFe_{12}O_{19}$ magnetic hard ferrites and $NiFe_2O_4$ spinel magnets [13,14] in a sufficient amount (as confirmed by the XRD analysis shown above). At the same

time, the coercivity of the BBFO ceramic decreases to 1.6 kOe, when it is impregnated with Ni.

4. Conclusions

A multiferroic $Bi_{0.75}Ba_{0.25}Fe_{0.975}Ni_{0.025}O_3$ solid solution was synthesized by the sol–gel method (without secondary phases). This multiferroic material, with maximum octahedral site Ni^{2+} cation substitution, exhibited enhanced ferromagnetic and ferroelectric properties. Ni acts as a grain growth inhibitor. It also reduces the grains coalescence. The magnetic properties were in a good agreement with those from the octahedral substitution. However, the ferroelectric profile showed a remanent polarization decrease from the original BBFO non-doped perovskite. In conclusion, there is an interesting compromise between ferromagnetic and ferroelectric properties in Ni doped perovskites.

Acknowledgments

The authors would like to thank Wilber Antunez, Carlos Santillan and Daniel Lardizábal for their valuable participation in this work. This work was supported by Project CONACYT no. 102171, as well as the Project “Estudio de cerámicas de Aurivillius con característicasferroicas” from the Facultad de Ciencias Quimicas, UACH.

References

[1] J.R. Teague, R. Gerson, W.J. James, Dielectric hysteresis in single crystal $BiFeO_3$, Solid State Communications 8 (1970) 1073–1074.
[2] N.A. Hill, Why are there so few magnetic ferroelectrics? Journal of Physical Chemistry B 104 (2000) 6694–6709.
[3] D.H. Wang, W.C. Goh, M. Ning, C.K. Ong, Effect of Ba doping on magnetic, ferroelectric, and magnetoelectric properties in mutiferroic $BiFeO_3$ at room temperature, Applied Physics Letters 88 (2006) 212907-3.
[4] A.R. Makhdoom, M.J. Akhtar, M.A. Rafiq, M.M. Hassan, Investigation of transport behavior in Ba doped $BiFeO_3$, Ceramics International 38 (2012) 3829–3834.
[5] S.K. Singh, R. Palai, K. Maruyama, H. Ishiwara, Effects of Ni substitution on structural, dielectrical, and ferroelectric properties of chemical-solution-deposited multiferroic $BiFeO_3$ films, Electrochemical and Solid-State Letters 11 (2008) G30–G32.
[6] X. Qi, J. Dho, R. Tomov, M.G. Blamire, J.L. MacManus-Driscoll, Greatly reduced leakage current and conduction mechanism in aliovalent-ion-doped $BiFeO_3$, Applied Physics Letters 86 (2005) 062903 062903.
[7] O.D. Jayakumar, S.N. Achary, K.G. Girija, A.K. Tyagi, C. Sudakar, G. Lawes, R. Naik, J. Nisar, X. Peng, R. Ahuja, Theoretical and experimental evidence of enhanced ferromagnetism in Ba and Mn cosubstituted $BiFeO_3$, Applied Physics Letters 96 (2010) 032903 032903.
[8] JCPDS-International Centre for Diffraction Data, Copyright (c) JCPDS-ICDD 2008, 01-089-8407.
[9] D.K. Mishra, X.D. Qi, Energy levels and photoluminescence properties of nickel-doped bismuth ferrite, Journal of Alloys and Compounds 504 (2010) 27–31.
[10] T.-J. Park, G.C. Papaefthymiou, A.J. Viescas, A.R. Moodenbaugh, S. S. Wong, Size-dependent magnetic properties of single-crystalline multiferroic $BiFeO_3$ nanoparticles, Nano Letters 7 (2007) 766–772.
[11] P. Singh, J.H. Jung, Effect of oxygen annealing on magnetic, electric and magnetodielectric properties of Ba-doped $BiFeO_3$, Physica B 405 (2010) 1086–1089.
[12] A. Gautam, V.S. Rangra, Effect of Ba ions substitution on multiferroic properties of $BiFeO_3$ perovskite, Crystal Research and Technology 45 (2010) 953–956.
[13] S. Castro, M. Gayoso, J. Rivas, J.M. Greneche, J. Mira, C. Rodríguez, Structural and magnetic properties of barium hexaferrite nanostructured particles prepared by the combustion method, Journal of Magnetism and Magnetic Materials 152 (1996) 61–69.
[14] P. Sivakumar, R. Ramesh, A. Ramanand, S. Ponnusamy, C. Muthamizhchelvan, Synthesis and study of magnetic properties of $NiFe_2O_4$ nanoparticles by PVA assisted auto-combustion method, Journal of Materials Science: Materials in Electronics 23 (2012) 1011–1015.